

## RAD-seq reveals Cenozoic shifts in the palaeogeographic distribution of *Trigonobalanus verticillata* across the Indochina Peninsula and Malay Archipelago<sup>☆</sup>

Ling Hu <sup>a,b,c,i</sup>, Pei-Han Huang <sup>a,d,i</sup>, Yi-Gang Song <sup>d</sup>, Shook Ling Low <sup>e,j</sup>, Guo-Xiong Hu <sup>f</sup>, Shi-Shun Zhou <sup>h</sup>, Lang Li <sup>a</sup>, Yun-Hong Tan <sup>h</sup>, Hong-Hu Meng <sup>a,h,\*</sup>, Yu-Peng Cun <sup>g,\*\*</sup>, Jie Li <sup>a,\*</sup>

<sup>a</sup> Plant Phylogenetics and Conservation Group, Center for Integrative Conservation & Yunnan Key Laboratory for Conservation of Tropical Rainforests and Asian Elephants, Xishuangbanna Tropical Botanical Garden, Chinese Academy of Sciences, Kunming 650223, China

<sup>b</sup> Institute of International Rivers and Eco-security, Yunnan University, Kunming 650500, China

<sup>c</sup> Southwest United Graduate Schools, Kunming 650092, China

<sup>d</sup> Eastern China Conservation Centre for Wild Endangered Plant Resources, Shanghai Chenshan Botanical Garden, Shanghai 201602, China

<sup>e</sup> Institute of Botany, Czech Academy of Sciences, 25243 Práhonice, Czech Republic

<sup>f</sup> College of Life Sciences, Guizhou University, Guiyang 550025, China

<sup>g</sup> Pediatric Research Institute, Ministry of Education Key Laboratory of Child Development and Disorders, National Clinical Research Center for Child Health and Disorders, China International Science and Technology Cooperation Base of Child Development and Critical Disorders, Chongqing Key Laboratory of Translational Medical Research in Cognitive Development and Learning and Memory Disorders, Children's Hospital of Chongqing Medical University, Chongqing 400014, China

<sup>h</sup> Southeast Asia Biodiversity Research Institute, Chinese Academy of Sciences, Naypyidaw 05282, Myanmar

<sup>i</sup> University of Chinese Academy of Sciences, Beijing 100049, China

<sup>j</sup> Forest Biodiversity Division, Forest Research Institute Malaysia, Kepong 52109, Selangor, Malaysia

### ARTICLE INFO

Editor: Howard Falcon-Lang

#### Keywords:

Paleogeography

Climate refugia

*Trigonobalanus verticillata*

Malay Archipelago

Indochina Peninsula

### ABSTRACT

The complex geological history and rich biodiversity of Southeast Asia have long fascinated biologists, ecologists, and biogeographers. In this paper, we address the spatiotemporal patterns of genetic diversity and dispersal dynamics of *Trigonobalanus verticillata* across the Indochina Peninsula and Malay Archipelago since the early Cenozoic and project distribution range shifts into the future. Our work is based on the integration of RAD-seq data with ecological niche modeling, to assess genetic diversity, genetic structure, divergence timing, and demographic dynamics. The key findings are as follows: (1) the species originated in north Sundaland, i.e., Indochina Peninsula, in the late Eocene, followed by Oligocene-Miocene stepwise south and northward dispersal events, establishing allopatric lineages via the Indochina Peninsula to the Yunnan and Hainan Island, while also expanding across Borneo to other regions of the Malay Archipelago. (2) Tectonically-driven habitat heterogeneity and inter-refugial gene flow promoted high genetic diversity in the Indochina Peninsula, whereas historical bottlenecks reduced genetic diversity in the Malay Archipelago. (3) Borneo served as a persistent region of refugial suitability from the Last Glacial Maximum to the present and is expected to retain its refugial function in the future. Our findings elucidate how Neogene-Quaternary environmental changes shaped contemporary biodiversity patterns in Southeast Asia, underscoring Borneo's critical role in conservation being a long-term refuge that has sustained the evolutionary potential of the species. Our integrative approach also provides a framework for understanding regional biogeographic dynamics through the genomic-level history of *T. verticillata*.

<sup>☆</sup> This article is part of a Special issue entitled: 'Genomic palaeoecology' published in Palaeogeography, Palaeoclimatology, Palaeoecology.

\* Corresponding author at: Plant Phylogenetics and Conservation Group, Center for Integrative Conservation & Yunnan Key Laboratory for Conservation of Tropical Rainforests and Asian Elephants, Xishuangbanna Tropical Botanical Garden, Chinese Academy of Sciences, Kunming 650223, China.

\*\* Corresponding author.

E-mail addresses: menghonghu@xtbg.ac.cn (H.-H. Meng), cunyp@cqmu.edu.cn (Y.-P. Cun), jieli@xtbg.ac.cn (J. Li).

## 1. Introduction

The Indochina Peninsula and Malay Archipelago are situated at the convergent boundary of the Eurasian, Indo-Australian, and Philippine plates (Hall, 2009, 2012, 2013; Meng and Song, 2023), and contain UNESCO-designated biodiversity hotspots of global conservation priority, including Indochina, Sundaic, Wallacea, and Philippines (Kellee, 2016; Meng and Song, 2023). This distinct biogeographical pattern was shaped by long-term interactions between ongoing plate tectonics, Quaternary climate oscillations and biogeographic filter effects as demonstrated by many phylogenetic studies (Buerki et al., 2014; Gao et al., 2023; Morley, 2018; Tan et al., 2020; Whittaker et al., 2017; Zhang et al., 2023, 2024).

The continental core of Sundaland originated from Gondwanan terranes that drifted northward and accreted to form Sundaland during the Cenozoic (Hall, 2009; Gao et al., 2024). In the Early Cenozoic, the collision between Indo-Eurasia induced rapid crustal thickening and orogenic uplift across the Indochina Peninsula, driving large-scale tectonic extrusion (Hall, 2013; Metcalfe, 2013). In the Oligocene, significant seafloor spreading began in the South China Sea, reorganizing regional drainage systems (Li et al., 2020). By the Miocene, the rapid uplift of the Himalayas intensified the emergence of the Asian monsoon system, and regular seasonal alternation of dry and wet had a significant impact on the rapid differentiation and spread of plants in Southeast Asia (Jiang et al., 2017; Meng et al., 2022). Quaternary glacial-interglacial cycles repeatedly exposed the Sunda Shelf during lowlands through sea-level fall events of c. 120 m amplitude, and established transient land bridges that modulated species dispersal dynamics via dispersal and diversification across the region (Husson et al., 2020; Voris, 2000). These geodynamic and paleoclimatic processes have profoundly shaped the region's exceptional physiographic complexity and environmental heterogeneity in Asia, mainly concentrated in East Asia and Southeast Asia (Li et al., 2025; Meng et al., 2025; Zhang et al., 2025).

In recent decades, phylogenetic investigations have significantly advanced our understanding of biogeographic history of Southeast Asia and adjacent regions through the studies of regional taxa (Huang et al., 2024, Huang et al., 2025; Meng et al., 2022; Quek et al., 2007; Zhang et al., 2025). Multi-taxon analyses, which include plants, amphibians, reptiles, arthropods, mammals, and birds have provided valuable insights into the complex evolutionary history across the regions (Che et al., 2010; Lim et al., 2020; Luo et al., 2023; Luo and Li, 2018, 2022; Mays et al., 2018; Shaney et al., 2020; Wurster et al., 2010; Zhang et al., 2025). Nevertheless, persistent sampling gaps and uneven geographical coverage continue to hinder the comprehensive synthesis of regional biogeographic dynamics. Furthermore, compared with fauna studies, datasets from plant studies that are suitable for multi-taxon integrative analyses remain comparatively limited (Lim et al., 2020). Therefore, before conducting integrative analyses on multi-taxon, it is urgent to carry out targeted studies on single-taxon to fill in the key data gaps. Compounding these research challenges, Southeast Asia's biodiversity faces unprecedented threats from anthropogenic pressures including habitat fragmentation, climate change-induced range shifts, and accelerating deforestation rates (Hughes, 2017). In this context, identifying and preserving potential climate refugia-areas demonstrating both historical persistence and future environmental stability-emerges as a critical conservation priority for safeguarding the region's unique biota.

*Trigonobalanus verticillata* (Fagaceae), a tropical evergreen tree that was initially recorded solely in Indonesia and Malaysia, has undergone significant range reassessment in 21st century. In 2005, a botanical survey conducted by Kadoorie Farm & Botanic Garden (Hong Kong, China) confirmed the presence of *T. verticillata* in Yinggeling, Hainan Province (Meng et al., 2019). Subsequent fieldwork in 2016, by researchers from the Xishuangbanna Tropical Botanical Garden of the Chinese Academy of Sciences extended its known distribution to Xishuangbanna, Yunnan Province (Meng et al., 2019). These discoveries

fundamentally altered understanding of the species' phytogeography and stimulated renewed investigation into its evolutionary history. At present, the species is known to spans three biodiversity hotspots in Southeast Asia (Indochina, Sundaic, and Wallacea; see Fig. S1), making it represent a potential model system for examining the region's biogeographic and evolutionary processes across the region's complex geographic background.

This study implemented a comprehensive range-wide sampling strategy for *T. verticillata*, coupled with restriction site-associated DNA sequencing (RAD-seq) to elucidate (1) fine-scale patterns of genetic diversity and population structure across the Indochina Peninsula and Malay Archipelago among disjunct populations using genome-wide SNP markers; (2) historical biogeographic trajectories through time-calibrated phylogenetic reconstruction through coalescent-based demographic analysis; and (3) potential Last Glacial Maximum (LGM) refugia using ecological niche modeling under paleoclimatic scenarios.

## 2. Material and methods

### 2.1. Sampling and RAD sequencing

More and more RAD-seq sequencing analyses were used in phylogeny and biogeography in recent years (Su et al., 2023; Zhao et al., 2023). Accordingly, we collected 85 individuals of *T. verticillata* from ten locations across Southwest China, the Indochina Peninsula, Malaysia, and Indonesia between 2017 and 2021 (Table 1; Fig. 1a). Sampling covered the entire known distribution range of the species. Genomic DNA was extracted using a Plant Genomic DNA Kit (Tiangen Biotech, Beijing, China). RAD-seq libraries were constructed by Shanghai Majorbio Biopharm Technology Co., Ltd. Genomic DNA was digested using the restriction enzyme *EcoRI*, and sequencing was performed on the Illumina NovaSeq 6000 platform with 150 bp paired-end (PE) reads.

### 2.2. RAD-seq analysis

We conducted quality control of the raw data using FastQC (<https://www.bioinformatics.babraham.ac.uk/projects/fastqc>) and Fastp (<http://github.com/OpenGene/fastp>). skrTools (<https://github.com/sharkLoc/skrTools>) was used to calculate the number of reads, GC content and average reads quality (Q30). Clean reads were processed to generate single nucleotide polymorphisms (SNPs) using Stacks v2.6 (Catchen et al., 2013). Specifically, we used the process *radtags* module with parameters -c -q -t 140 to discard low-quality reads and ambiguous bases, and trim reads to 140 bp. We mapped filtered reads from all individuals to the *Castanea mollissima* reference genome (GCA\_014183005.1, Wang et al., 2020) using BWA-MEN v0.7.17 (Li, 2013) with the parameters -t 24 -M. Mapped reads were sorted and converted into BAM format using SAMtools (Li et al., 2009). Then, we constructed loci from the aligned paired-end data using the *gstacks* module in Stacks, followed by SNP calling and filtering using the *populations* module. To ensure high-quality variant data, we applied stringent filtering criteria during SNP calling. We retained loci that were present in at least 80 % of individuals within each population (-r 0.8) and shared across all ten populations. To avoid bias introduced by linkage disequilibrium, we retained only the first SNP per locus. Loci with a minimum allele frequency (MAF) below 0.05 were excluded, and the maximum observed heterozygosity was set to 0.5 to ensure the reliability of population structure inference.

### 2.3. Genetic diversity

The *populations* module in Stacks was used to estimate expected heterozygosity ( $H_e$ ), observed heterozygosity ( $H_o$ ), inbreeding coefficient ( $F_{IS}$ ), nucleotide polymorphism ( $P_i$ ), and pairwise genetic distance ( $F_{ST}$ ). To access genetic variation at hierarchical levels (among groups, among populations, and within populations), we performed an analysis

**Table 1**  
Sampling information of *T. verticillata*.

| Population | Location                               | Longitude     | Latitude     | Elevation(m) | (N) |
|------------|--|---------------|--------------|--------------|-----|
| LD         | Vietnam                                | 108°33'9"     | 12°06'11"    | 1491         | 16  |
| KPD        | Vietnam                                | 108°15'45"    | 14°35'42"    | 1193         | 11  |
| YGL        | Yinggeling, Hainan                     | 109°22'41"    | 18°58'23"    | 996          | 5   |
| BLS        | Bulang Mountain, Xishuangbanna, Yunnan | 100°26'21.60" | 22°35'19.20" | 1179         | 8   |
| TWA        | Sumatra, Indonesia                     | 100°25'8.61"  | 0°2'56.74"   | 636          | 6   |
| MM         | Sulawesi, Indonesia                    | 119°16'13.90" | 2°33'16.30"  | 1448         | 1   |
| FJ         | Fraser's hill, Malaysia                | 101°42'41.34" | 3°43'39.72"  | 954          | 12  |
| GJ         | Kuching, Malaysia                      | 110°13'13"    | 1°7'10.86"   | 954          | 7   |
| BA         | Bario, Malaysia                        | 115°29'43.8"  | 3°44'14.58"  | 1207         | 10  |
| LR         | Lawas, Malaysia                        | 115°35'15.24" | 4°6'37.62"   | 1276         | 9   |
| Total      |  |               |              |              | 85  |

of molecular variance (AMOVA) using Arlequin v3.5.2 (Excoffier and Lischer, 2010). Input file formats were converted using PGDspider v 2.1.1.5 (Lischer and Excoffier, 2012). Wu used  $F_{ST}$  to quantify genetic distances among populations and calculated geographical distances among populations using the *geosphere* package (Hijmans, 2024). To test isolation and distance (IBD), we performed the Mantel test using *mantel.randtest()* function from *ade4* package (Dray et al., 2007), evaluating the correlation between genetic distance and geographical distance.

#### 2.4. Population structure and gene flow

We assessed the genetic structure using ADMIXTURE (Alexander et al., 2009), testing values of  $K$  (number of genetic clusters) from 1 to 10, with 10 repetitions for each  $K$ . The optimal number of clusters was determined using StructureSelector (Li and Liu, 2018), based on 10-fold cross-validation error. The final population structure was visualized using CLUMPAK (Kopelman et al., 2015). Principal component analysis (PCA) was performed using PINK (Purcell et al., 2007), and the first two PCs (PC1, PC2) were visualized using the *ggplot2* package in R (Wickham, 2016). Although the use of  $F_{ST}$  to estimate gene flow ( $Nm$ , the number of migrants successfully entering a population per generation) has known limitations, it still offers a rough approximation under certain conditions (Whitlock and McCauley, 1999). Therefore, we estimated species-level gene flow using the formula  $Nm = (1-F_{ST})/(4 \times F_{ST})$ , while acknowledging the assumptions and limitations of this approach (Whitlock and McCauley, 1999). To better infer the migration events among populations, we used TreeMix v1.13 (Pickrell and Pritchard, 2012). TreeMix first constructs a maximum likelihood tree of the sampled populations, and then models the migration events superimposed on this tree. We allowed up to six migration events and used the “-noss” parameter to avoid sample size over-correction. The optimal number of migration edges was identified using the *OptIM* package (Fitak, 2021). Visualization of the migration tree and heatmap was performed using R script *plotting\_funcs.R* ([https://github.com/joepickrell/pophistory-tutorial/blob/master/example2/plotting\\_funcs.R](https://github.com/joepickrell/pophistory-tutorial/blob/master/example2/plotting_funcs.R)).

#### 2.5. Divergence time estimation and biogeographical analyses

A maximum likelihood tree was inferred using RAxML v8.2.12 (Stamatakis, 2014) under GTRGAMMA nucleotide substitution model with 1000 bootstrap iterations. Meanwhile, *T. doichangensis*, *Fagus longipetiolata*, and *F. hayatae* were used as outgroups. To estimate divergence times among lineages more accurately, we first used the *populations* module in Stacks to obtain population-level genetic variation data. A population tree was constructed to estimate divergence time. The divergence time was performed using BEAST v1.10.4 (Suchard et al., 2018) based on a Bayesian MCMC algorithm. We applied a lognormal relaxed molecular clock model and a Yule process tree prior. All parameters were set in BEAUTi v1.10.4, with the MCMC chain run for  $3 \times 10^8$  generations, sampling every  $2 \times 10^4$  generations. Convergences

were monitored using Tracer v1.7.2 (Rambaut et al., 2018), ensuring that the effective sample size (ESS) value exceeded 200 for all parameters. A maximum clade credibility tree was generated using TreeAnnotator v1.10.4.

We employed two fossil calibration points based on the Fagaceae phylogeny. (i) The staminate inflorescence fossils *Trigonobalanoid* sp. 1 and *Trigonobalanoid* sp. 2, reported from Baltic amber (33.9–37.8 Ma), which exhibit features resembling extant *T. verticillata*, were used to calibrate the crown age of *Trigonobalanus* (Sadowski et al., 2020). (ii) The pollen fossil *Fagoideae* from the Campanian of Wyoming (81–82 Ma) was used to calibrate the stem age of *Trigonobalanus* (Grímsson et al., 2016).

To infer the historical geographic distribution of *T. verticillata*, we performed ancestral state reconstruction using RASP v4.3 (Yu et al., 2019) on the dated phylogeny. Geographic regions were coded based on distribution patterns: (A) Borneo; (B) South and southwest China; (C) Malaysia Peninsular and Sumatra; (D) Indochina Peninsula (along the Truong Son Mountains (Mts.)); and (E) Sulawesi. We applied the statistical dispersal-extinction-cladogenesis (S-DEC) model in RASP.

#### 2.6. Demographic history

To investigate the recent demographic history of *T. verticillata*, all populations were grouped according to the results of the genetic structure analysis, and ANGSD (Korneliussen et al., 2014) was used to generate the unfolded site frequency spectrum. Demographic inference was performed using Stairway Plot v2.1.2 (Liu and Fu, 2020), which estimates changes in historical effective population size. Based on previous study in *Castanea* (Nie et al., 2024), we assume an average mutation rate of  $5.2 \times 10^{-8}$ , and an average generation time of 15 years for *T. verticillata*.

#### 2.7. Ecological niche modeling

Species occurrence data for *T. verticillata* were compiled from the Global Biodiversity Information Facility (GBIF, <https://www.gbif.org/>), the Kew Royal Botanic Garden herbarium database (<http://apps.kew.org/herbcat/gotoHomePage.do>), and field sampling points from this study. To mitigate spatial sampling bias and prevent model overfitting, occurrence records were spatially thinned at a 10 km using SDMtools in ArcGIS v10.7 (Hu et al., 2025). Environmental data were obtained from WorldClim (<https://www.worldclim.org>), which includes 19 bioclimatic variables for the Last Glacial Maximum (LGM; ca. 22kya before present), the Mid Holocene (MIH; ca. 6kya before present), the current period (1970–2000), and two future projections (2041–2060; 2061–2080). The spatial resolution was 2.5 arcmin. Future projections were based on the Representative Concentration Pathway RCP4.5. To avoid multicollinearity, we conducted a correlation analysis of the 19 bioclimatic variables in ArcGIS and excluded highly correlated variables ( $|r| \geq 0.8$ ) (Table S3). Ecological niche modeling (ENM) was performed using MAXENT v3.4.1 (Elith et al., 2011). Twenty percentage of the

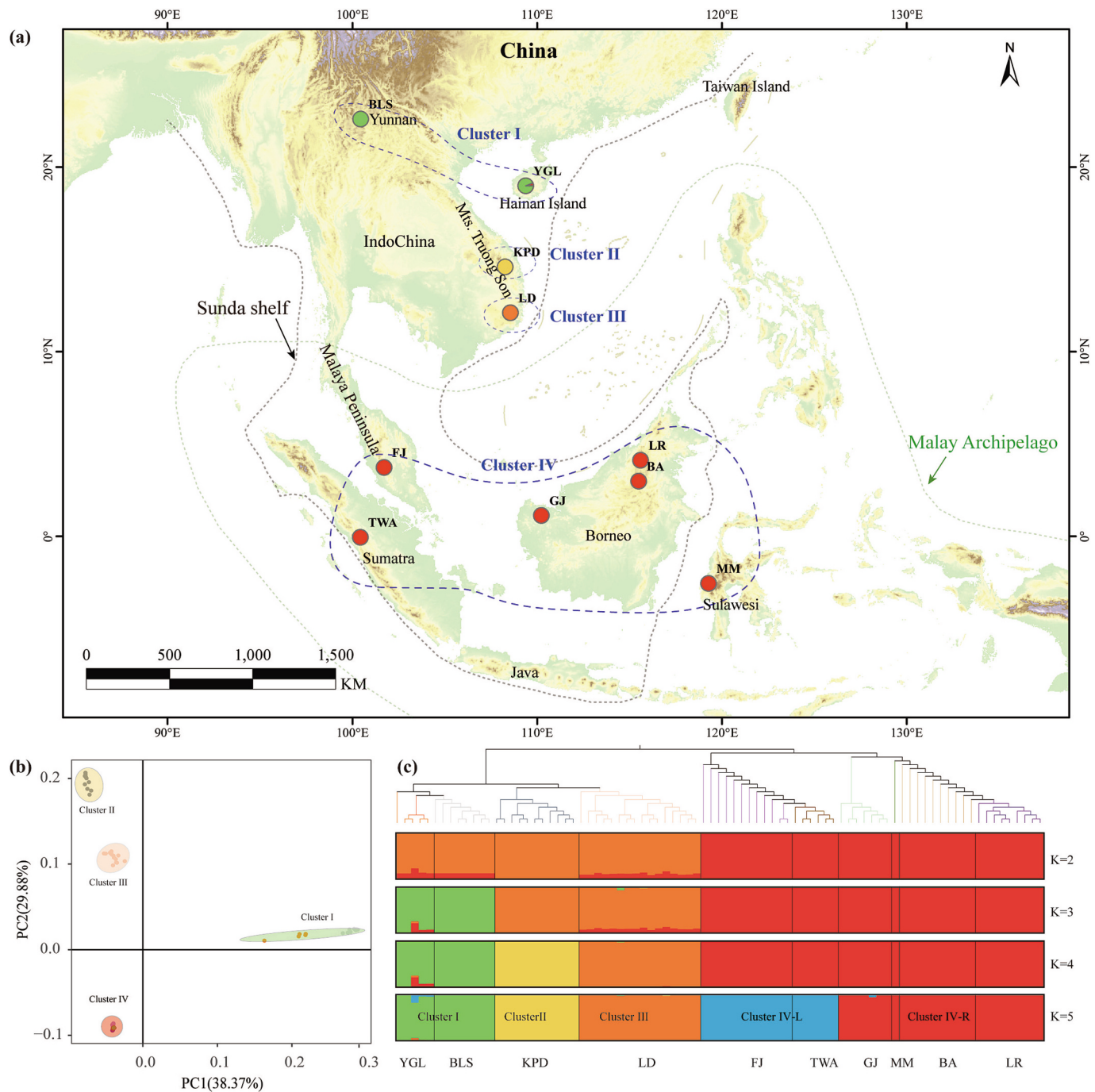


**Fig. 1.** Geographical distribution and population genetic structure of *T. verticillata*. (a) Geographical distribution of the 85 sampled populations and their color-coded grouping according to the structure analysis ( $K = 4$ ). Sunda shelf and Malay Archipelago were modified from Meng and Song, 2023. (b) Principal component analysis (PCA) plot generated for the *T. verticillata* population. (c) Histogram of the structural analysis for the model with  $K = 2$ ,  $K = 3$ ,  $K = 4$ , and  $K = 5$ .

occurrence data were randomly selected as a test set. The model was run with a maximum of 1000 iterations, and 10 repetitions were run to ensure robustness (Hu et al., 2025). Model performance was evaluated using the area under the receiver operating characteristic curve (AUC), and potential distribution maps for different periods were visualized in ArcGIS. A 10 % training presence cloglog threshold was used to classify habitat suitability: low suitability (threshold-0.6), medium suitability (0.6–0.8), and high suitability (0.8–1) (Hu et al., 2025).

### 3. Results

#### 3.1. RAD sequences

Following strict quality control of RAD sequencing data, a total of 215.36 G of high-quality data was obtained, with an average GC content of 36.98 %, and the Q30 was 91.71 %.

Two datasets were generated after filtering using *populations* module. The first dataset contained all 85 *T. verticillata* individuals and retained 24370 SNPs for subsequent genetic structure analysis. The second dataset incorporated three outgroup species, *T. doichangensis*, *F. longipetiolata*, and *F. hayatae*, and contained 2409 SNPs for

phylogenetic reconstruction and divergence time estimation.

### 3.2. Genetic structure and phylogenetic relationships

Results from ADMIXTURE and PCA analyses revealed four distinct genetic lineages (Fig. 1, S2). Cluster I is distributed in Yunnan and on Hainan Island (Fig. 1, green). Cluster II is confined to the central part of the Truong Son Mts. range (Fig. 1, yellow), whereas cluster III is found in the southern part of the Truong Son Mts. range, with both cluster II and III occupying different elevations along the range (Fig. 1, orange).

Although cluster IV appeared genetically homogeneous in the ADMIXTURE analysis, phylogenetic reconstruction revealed a more complex pattern. Within cluster IV, populations FJ and TWA formed one clade, while GJ, MM, BA, and LR grouped into a separate clade (Fig. 2b). Based on this clear phylogeographic structure, we further subdivided Cluster IV into two sub-lineages: cluster IV-L and cluster IV-R (Fig. 1c). These findings suggest the presence of four genetically structured lineages within *T. verticillata*, with evidence of finer-scale divergence in some regions, particularly within the Malay Archipelago.

### 3.3. Divergence time estimates and biogeographical analyses

Divergence time estimates revealed key evolutionary events in the history of *T. verticillata*. The stem age of *T. verticillata* was estimated to be ca. 36.12 Ma, during the late Eocene (95 % HPD: 34.20–38.06 Ma). Internal diversification within *T. verticillata* began at ca. 25.24 Ma (95 % HPD: 32.87–16.05 Ma), coinciding with the formation of cluster IV (Fig. 2b; Table 3). Cluster I diverged at ca. 18.96 Ma (95 % HPD: 27.97–9.68 Ma), while clusters II and III split at ca. 7.37 Ma (95 % HPD: 16.52–0.24 Ma) (Fig. 2b; Table 3). Within cluster IV, the divergence between sub-cluster IV-L and IV-R occurred at ca. 13.19 Ma (95 % HPD: 24.70–2.32 Ma) (Fig. 2b; Table 3).

Biogeographical reconstruction using the S-DEC model suggested that *T. verticillata* originated in Sundaland. Subsequent divergence

events resulted in two major lineages (Fig. S3). Our results indicate that four vicariance and three dispersal events occurred from the Oligocene to the Miocene (Fig. S3). Ancestral lineages appear to have persisted in Indochina, followed by northward expansion into Yunnan and Hainan Island, and southward to Borneo. This was later accompanied by radiation and dispersal across most of the Malay Archipelago (Fig. 2b; S3).

### 3.4. Genetic diversity

Genetic diversity analysis across 10 *T. verticillata* populations revealed substantial variation. The observed heterozygosity ( $H_o$ ) ranged from 0.0292 to 0.2115, expected heterozygosity ( $H_e$ ) ranged from 0.0146 to 0.2028, and nucleotide diversity ( $P_i$ ) ranged from 0.0274 to 0.2097. The inbreeding coefficient ( $F_{IS}$ ) varied from -0.0491 to 0.02 (Table 2). The genetic differentiation coefficient ( $F_{ST}$ ) ranged from 0.0326 to 0.4176, with an average value of 0.208 (Table S1).

AMOVA revealed that majority of the genetic variation occurred among populations ( $F_{ST} = 0.5192$ ) (Table S2). ADMIXTURE results further indicated that 55.45 % of the genetic variation was partitioned among groups, whereas only 3.58 % occurred among populations within

**Table 2**  
The genetic diversity parameters.

| POP_ID | $H_o$  | $H_e$  | $P_i$  | $F_{IS}$ |
|--------|--------|--------|--------|----------|
| BLS    | 0.1554 | 0.1427 | 0.1526 | -0.0034  |
| YGL    | 0.1583 | 0.1393 | 0.1555 | -0.0037  |
| LD     | 0.2031 | 0.2028 | 0.2097 | 0.0200   |
| KPD    | 0.2115 | 0.1802 | 0.1891 | -0.0491  |
| BA     | 0.0335 | 0.0261 | 0.0276 | -0.0141  |
| FJ     | 0.0385 | 0.0310 | 0.0325 | -0.0152  |
| GJ     | 0.0340 | 0.0263 | 0.0285 | -0.0126  |
| LR     | 0.0330 | 0.0259 | 0.0275 | -0.0129  |
| TWA    | 0.0348 | 0.0249 | 0.0274 | -0.0150  |
| MM     | 0.0292 | 0.0146 | 0.0292 | 0.0000   |

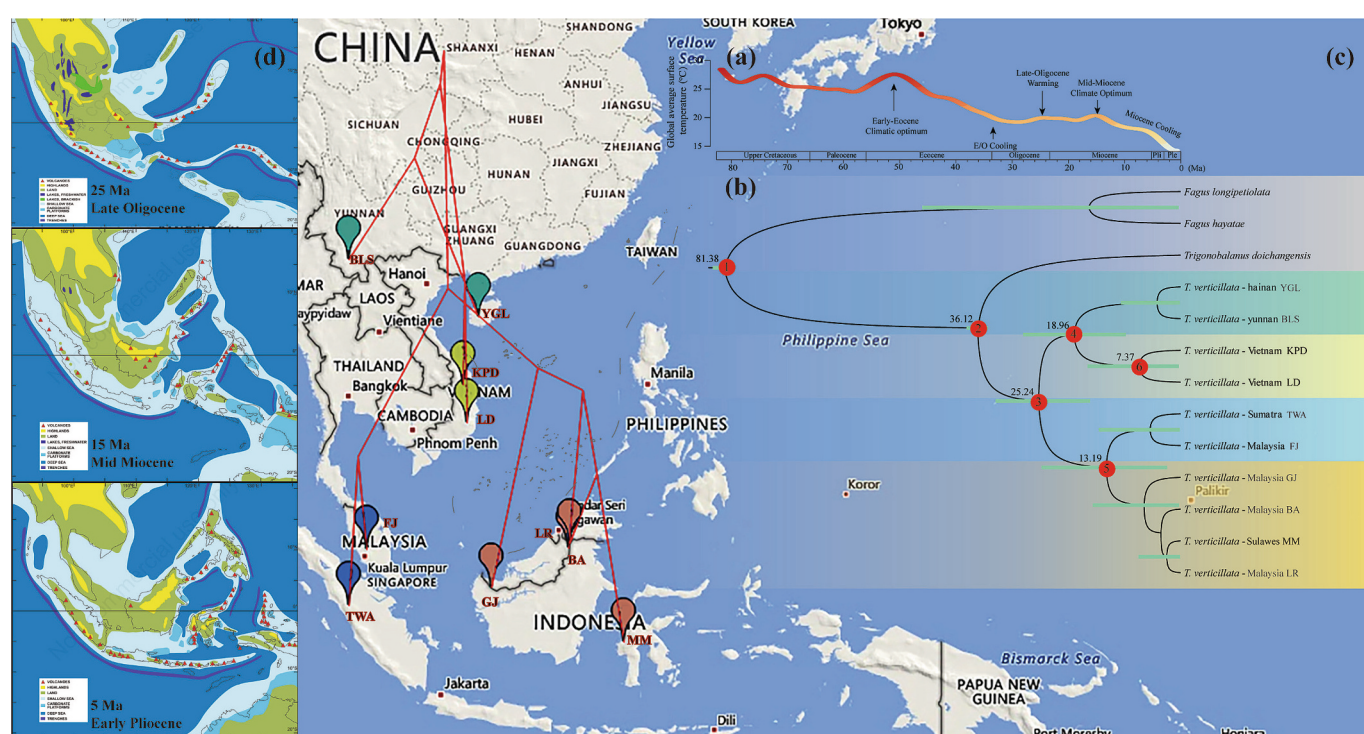


**Fig. 2.** (a) The global climate curve during the last 82 million years, major climate events were indicated (from Zhou et al., 2022). Ma, millions of years ago; Pli, Pliocene; Ple, Pleistocene. (b) Chronogram of *T. verticillata* inferred by BEAST. Green bars on nodes represent the 95 % highest posterior density estimates. (c) A phylogeographic tree generated using PGT according to the approach (Xia, 2019). (d) Paleogeography of Southeast Asia in the Late Oligocene, Mid Miocene, and Early Pliocene (from Hall, 2013). (For interpretation of the references to color in this figure legend, the reader is referred to the web version of this article.)

**Table 3**

Mean age and 95 % highest posterior density (HPD) estimates in million years ago (Ma).

| Node                       | Mean age and 95 % highest posterior density (HPD) estimates |
|----------------------------|---|
| 1–Fossil calibration point | 81.38 (83.28–79.39) Ma                                      |
| 2–Fossil calibration point | 36.12 (38.06–34.20) Ma                                      |
| 3                          | 25.24 (32.87–16.05) Ma                                      |
| 4                          | 18.96 (27.92–9.68) Ma                                       |
| 5                          | 13.19 (24.70–2.32) Ma                                       |
| 6                          | 7.37 (16.52–0.24) Ma  |

groups. The Mantel test revealed a significant positive correlation between geographic and genetic distance ( $r = 0.5902$ ,  $p < 0.001$ , Fig. S5). The estimated gene flow ( $Nm$ ) across populations was relatively low at 0.9519 (Table S2). TreeMix analysis identified historical gene flow among the populations, with a migration event inferred from population GJ to populations TWA and FJ, having a migration weight of 0.1972 (Fig. S6).

### 3.5. Demographic history

We investigated the demographic history of *T. verticillata* across its major genetic lineages using a Stairway Plot. The results show that during the Last Glacial Period (LGP), cluster I underwent a pronounced population bottleneck, with a sharp decline in the effective population occurring at approximately 70–40 kya (Fig. 3). Clusters II and III also experienced reductions in effective population size during this period, which later stabilized post-glaciation (Fig. 3). In contrast, cluster IV maintained a relatively stable demographic history throughout the LGP (Fig. 3). However, cluster IV-L exhibited a significant contraction in effective population size during the LGM, whereas cluster IV-R showed no marked fluctuations, maintaining a stable demographic trend without evidence of contraction or expansion (Fig. S4).

Due to the limited number of species occurrence records, we conducted only a broad-scale ENM analysis. The ENM results suggest that the present-day distribution of *T. verticillata* is primarily concentrated in

Malaysia, Sumatra, and Borneo, which provide the most suitable habitats under current climatic conditions (Fig. 4c). During the LGM, the species exhibited a considerably broader distribution across Sumatra, Borneo, Sulawesi, and the Philippines (Fig. 4a). By the mid-Holocene, this range had begun to contract, with a noticeable shift in the distribution center. Limited range expansion was observed during this period in Sulawesi and the Truong Son Mts. (Fig. 4b). In the future, the potential distribution of this species will be primarily concentrated in Borneo and Sulawesi (Fig. 4d, e).

## 4. Discussion

### 4.1. Genetic diversity differentiation between Indochina Peninsula and Malay Archipelago

Our results revealed a clear pattern, with populations of *T. verticillata* in Indochina Peninsula exhibit significantly higher genetic diversity than those in the Malay Archipelago. One possible explanation for this disparity is the refugium effect. Our demographic analyses indicate notable contractions in effective population size during glacial periods in the central and southern Truong Son Mts. (Fig. 3). Therefore, high genetic diversity is likely the result of postglacial habitat recovery and gene flow among populations (Wielstra et al., 2021; Yi and Latch, 2022). Notably, although these populations formed two genetically distinct clusters (Fig. 1c), estimates of gene flow ( $Nm = 1.7958$ ) suggest substantial connectivity. This gene flow among Truong Son Mts. populations likely counteracts genetic drift while accumulating and maintaining substantial genetic variation (Wang et al., 2017). Importantly, the Truong Son Mts. in Indochina Peninsula have long been recognized as a glacial refugium in Southeast Asia, alongside the mountains of Southwest China (Zhang et al., 2021; Ziegler et al., 2019). These areas have functioned both as evolutionary museums and cradles for numerous endemic species (Huo and Sun, 2024; Loria et al., 2022), likely allowing *T. verticillata* populations in Truong Son Mts. to maintain contact and persist after disturbance, preserving high levels of genetic diversity (Zhang et al., 2021). Meanwhile, the complex topography and ecological heterogeneity of the Indochina Peninsula likely facilitated localized adaptation and population differentiation, further contributing to local genetic diversity (Ortego et al., 2015).

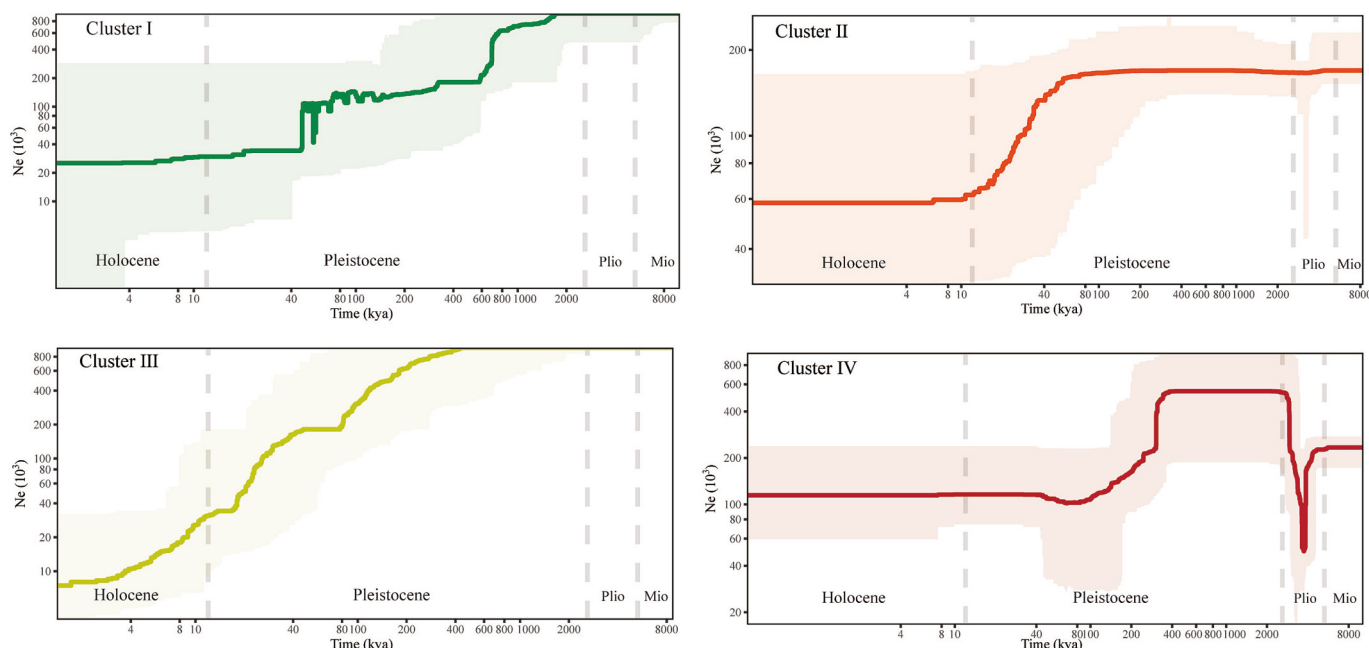


**Fig. 3.** Demographic history inferred by Stairway Plot for the four clusters of *T. verticillata*. The x-axis shows the time before the present (kya), and the y-axis reflects the effective population size. The bold colored curve indicates the median estimate and the shaded area represents the 95 % confidence interval.

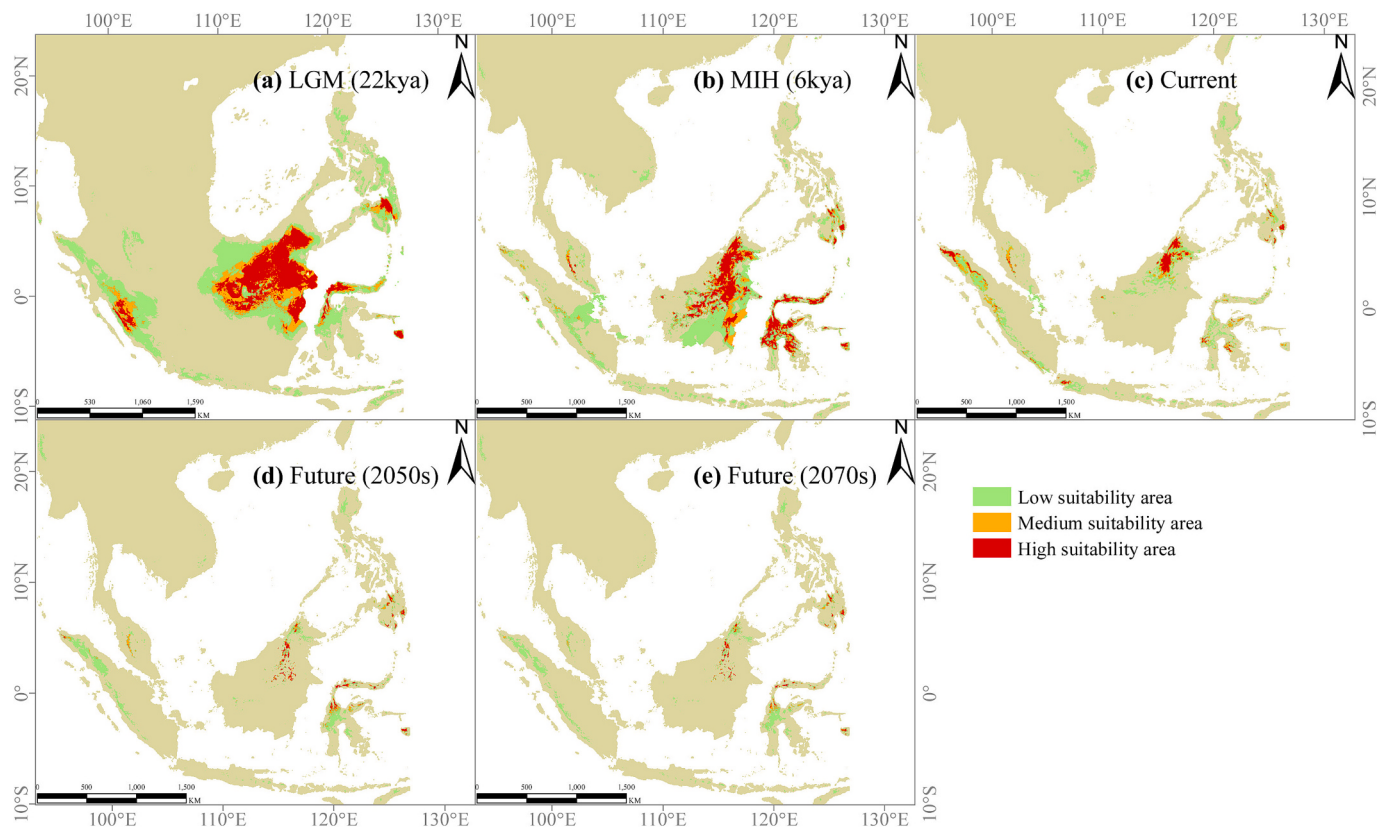


**Fig. 4.** Ecological niche modeling of *T. verticillata*. (a) The LGM, 22 kya before the present, (b) the MIH, 6 kya before the present, (c) current (1970–2000), (d, e) future 2050s (2041–2060) and 2070s (2061–2080). Low suitability (10 % training presence cloglog threshold-0.6), medium suitability (0.6–0.8), and high suitability (0.8–1).

In contrast, the low genetic diversity observed in Malay Archipelago appears to result from a combination of founder effects and genetic drift. Our demographic inference points to a pronounced historical bottleneck occurring between the late Miocene to the early Pliocene in the Malay Archipelago (Fig. 3). This timing coincides with the subsidence and marine transgression events of Sundaland, coupled with continued compression between the Australian and Sundaland plates, which triggered tectonic activity along the Banda Arc and the uplift of Sulawesi (Fig. 2d) (Hall, 2009; Lohman et al., 2011). These events likely caused population contractions and triggered founder effects. Subsequent small population sizes would have aggravated the effect of genetic drift, resulting in a rapid decrease in genetic diversity (Salgotra and Chauhan, 2023; Segelbacher et al., 2014; Wang et al., 2017). During the Pliocene (ca. 3 Ma), global cooling and sea-level drops temporarily reconnected the Indochina Peninsula, Hainan, Taiwan, Sumatra, Java, and Borneo, forming the Sundaland (Fig. 2a) (Meng and Song, 2023). We speculate that *T. verticillata* likely dispersed across parts of the Malay Archipelago during this time, leading to population expansion (Fig. S3). Migration events inferred from our data also support this scenario (Fig. S6). Nevertheless, the effects of the earlier bottleneck persisted, leaving the Malay Archipelago populations with long-term reduced diversity. Our analyses also suggest that vicariance was a primary cause for the pattern observed in the eastern and western parts of the Malay Archipelago (Fig. S3). This indicates that the diversification within cluster IV was largely driven by vicariance (Dixit et al., 2023; Li and Li, 2018).

Overall, topographic heterogeneity and inter-population gene flow in the Indochina Peninsula have maintained high genetic diversity and reduced the effects of genetic drift. In contrast, the population shrinkage in the late Miocene in the Malay Archipelago was shaped by geological isolation, bottleneck events, and limited connectivity. These findings underscore how ancient geological and climatic events continue to

shape present-day patterns of genetic diversity and provide valuable insights into the evolutionary dynamics underlying biodiversity maintenance in Southeast Asia.

#### 4.2. Formation history of the geographical pattern of *T. verticillata*

The complex geological history and repeated glacial sea-level fluctuations in Southeast Asia have profoundly influenced the biogeographic patterns and diversification of regional biota, including *T. verticillata*. During the Eocene to early Miocene, frequent volcanic activity along the southern margin of the Sunda Shelf reshaped the region's landscape (Hall, 2013). Meanwhile, the collision between the India and Eurasia plates, along with the opening of the South China Sea (Hall, 2013; Li et al., 2023), led to major geological transformations, significantly expanding the landmass of Sundaland (Crayn et al., 2015; Tang et al., 2024). This expanded land area may have acted as a terrestrial corridor for the dispersal of *T. verticillata* across parts of the Malay Archipelago (Fig. 2d). Sea-level fluctuations have been widely regarded as a central driver of high biodiversity in Southeast Asia. During periods of sea-level fall, the exposed Sundaland promoted connectivity among populations. This dynamic “species pump” effect has repeatedly fostered diversification and gene flow (Salles et al., 2021), a pattern strongly supported by our data.

Genetic structure analyses revealed distinct divergence between lineages in the Malay Archipelago and the Indochina Peninsula. Phylogenetic reconstructions indicate that the populations from southern China and the Truong Son Mts. diverged from those in the Malay Archipelago during the late Oligocene to early Miocene (Fig. 2b). This divergence coincides with high sea-levels in the middle Miocene, and the gradual flooding of northern and western Sunda Shelf likely restricted biotic exchange, thereby isolating populations in the Malay

Archipelago and the Indochina Peninsula (Fig. 2a, d; Hall, 2013; Morley, 1998). As global temperatures declined and sea-level dropped in the late Miocene and Pliocene, likely have opened a pathway for the exchange of *T. verticillata* from the Indochinese Peninsula to Peninsular Malaysia and Borneo. Numerous studies have confirmed that Sundaland experience repeated episodes of land exposure and submergence during the Quaternary, enabling the cyclical isolation and reconnection of populations (Hall, 2012; Hall, 2013; Husson et al., 2020, 2022). These events likely contributed to the accelerated diversification observed within *T. verticillata* lineages.

The genetic homogeneity observed among Malay Archipelago populations may reflect their historical connectivity via the exposed Sundaland. Paleogeographic studies suggest that Sundaland remained exposed until at least 400 kya (Husson et al., 2020). This evidence provides important insights into the close paleogeographic connections among the islands in Southeast Asia. This connectivity likely played a critical role in shaping evolutionary history of *T. verticillata*, underscoring the significance of periodic Sundaland exposure in shaping the history of biodiversity. Furthermore, our findings show that extant *T. verticillata* populations are now confined to high elevations habitats or mountain peaks (Fig. S1). This elevational distribution pattern may reflect the legacy of historical sea-level fluctuations, where rising sea-level isolated lowland regions as islands, causing population fragmentation, and ultimately forming the current distribution pattern (Li and Li, 2018).

#### 4.3. Climate change responses and potential refuge

Genetic diversity is a fundamental indicator of a species' adaptive capacity in the face of environmental change (Yu et al., 2021). Our results showed that *T. verticillata* harbors relatively low genetic diversity ( $Pi = 0.0274\text{--}0.2097$ ,  $He = 0.0146\text{--}0.2028$ ), which is markedly lower than its same genus *T. doichangensis* ( $Pi = 0.2504\text{--}0.3343$ ,  $He = 0.2232\text{--}0.3059$ ; Hu et al., 2022). Moreover, we observed strong genetic differentiation among populations of *T. verticillata*, with a significant positive correlation between genetic distance and geographic distance (Fig. S5). The fragmented geographic distribution of *T. verticillata* across multiple countries and regions, coupled with increasing anthropogenic pressures, including habitat loss due to development or policy requirements, has led to significant declines in individuals (Lin et al., 2007; Meng et al., 2019). These human-induced disturbances have likely exacerbated the loss of genetic variation, posing a considerable threat to the species (Meng et al., 2019, 2021).

The current geographic distribution and genetic patterns of *T. verticillata* are likely shaped by climatic fluctuations during the Pleistocene. Notably, during the LGP, populations in Yunnan, Hainan Island, and the Indochina Peninsula experienced significant demographic contractions, whereas populations in the Malay Archipelago remained relatively stable (Fig. 3). Particularly noteworthy was the rapid decline of subcluster IV-L during the LGP, contrasting with the stability of subcluster IV-R (Fig. S4). This differential response strongly supports the Borneo rainforest refugia hypothesis (Kuhnhäuser et al., 2025; Wurster et al., 2010).

Our findings indicate that Borneo served as a critical glacial refuge during the Quaternary, playing a pivotal role in preserving both the population structure and genetic diversity of *T. verticillata*. Ecological niche modeling further supports significant ecological niche shifts in *T. verticillata* from the LGM to the present. During the LGM, the distribution center of *T. verticillata* was located in Borneo and Sumatra, aligning with the location of cluster IV (Fig. 4a). Future projections suggest that the distributional center of *T. verticillata* is likely to remain in Borneo, reinforcing this region's role as a stable ecological buffer against climatic fluctuations (Fig. 4d, e). Since the middle Holocene, the distribution range of *T. verticillata* has shown both contraction and expansion, particularly into Sulawesi (Fig. 4b). However, ongoing land use changes and habitat degradation have caused further population

declines (Meng et al., 2019). The combination of low genetic diversity and increasing anthropogenic pressure threaten the species' viability (Table 2; Meng et al., 2019). In contrast, species with high genetic diversity and broader distributions exhibit higher adaptability to climate change (Hu et al., 2025).

In view of our findings, we suggest conservation efforts for populations of *T. verticillata* with high genetic diversity, which are essential to maintaining the species' evolutionary potential. Particular priority should be given to the Borneo region, which has acted as a key refugium since the LGM and is projected to remain vital for the species' future survival. Its ecological capacity is crucial for the survival of the species and must be prioritized for inclusion in the conservation network.

#### 5. Conclusion

In summary, our study reconstructs the evolutionary history of *T. verticillata* across the Indochina Peninsula and the Malay Archipelago. Our findings indicate that *T. verticillata* originated in Sundaland during the late Eocene, with major diversification events occurring between the late Miocene and the Pliocene. During the Oligocene to Miocene, *T. verticillata* expanded northward into the Yunnan and Hainan Island via dispersal from the Indochina Peninsula, while simultaneously spreading and radiating to Borneo and other parts of Malay Archipelago. We demonstrate that the high genetic diversity observed in the Indochina Peninsula was maintained by topographic heterogeneity and historical gene flow among refugia, whereas the low genetic diversity in the Malay Archipelago likely resulted from historical bottlenecks and prolonged isolation. Given that Borneo has always been an important refuge for *T. verticillata*, we believe that it is essential to prioritize this region in conservation efforts to mitigate the risk of local extinctions.

#### CRediT authorship contribution statement

**Ling Hu:** Writing – review & editing, Writing – original draft, Visualization, Software, Methodology, Investigation, Formal analysis, Data curation, Conceptualization. **Pei-Han Huang:** Writing – review & editing, Writing – original draft, Methodology. **Yi-Gang Song:** Writing – original draft. **Shook Ling Low:** Writing – review & editing, Resources. **Guo-Xiong Hu:** Writing – original draft. **Shi-Shun Zhou:** Writing – original draft, Investigation. **Lang Li:** Writing – original draft, Investigation. **Yun-Hong Tan:** Writing – original draft, Investigation. **Hong-Hu Meng:** Writing – review & editing, Writing – original draft, Supervision, Resources, Project administration, Investigation, Funding acquisition, Data curation, Conceptualization. **Yu-Peng Cun:** Writing – review & editing, Writing – original draft, Funding acquisition, Conceptualization. **Jie Li:** Writing – review & editing, Writing – original draft, Supervision, Resources, Project administration, Funding acquisition.

#### Declaration of competing interest

The authors declare no conflicts of interest.

#### Acknowledgments

This research was supported by the Yunnan Fundamental Research Projects (202301AT070341); the Special Fund for Scientific Research of Shanghai Landscaping & City Appearance Administrative Bureau (G242414, G242416); the Southeast Asia Biodiversity Research Institute, Chinese Academy of Sciences (No. Y4ZK111B01); the CAS "Light of West China"; the "Yunnan Revitalization Talent Support Program" in Yunnan Province (XDYC-QNRC-2022-0028); Yunnan Revitalization Talent Support Program "Innovation Team" Project (202405AS350019); and the 14th Five-Year Plan of Xishuangbanna Tropical Botanical Garden, Chinese Academy Sciences (XTBG-1450303).

## Appendix A. Supplementary data

Supplementary data to this article can be found online at <https://doi.org/10.1016/j.palaeo.2025.113291>.

## Data availability

The raw data of the RAD-seq generated in this study have been deposited in the National Genomics Data Center (NGDC, <https://ngdc.cncb.ac.cn>) under accession number PRJCA041353.

## References

- Alexander, D.H., Novembre, J., Lange, K., 2009. Fast model-based estimation of ancestry in unrelated individuals. *Genome Res.* 19 (9), 1655–1664. <https://doi.org/10.1101/gr.094052.109>.
- Buerki, S., Forest, F., Alvarez, N., 2014. Proto-South-East Asia as a trigger of early angiosperm diversification. *Bot. J. Linn. Soc.* 174 (3), 326–333. <https://doi.org/10.1111/bj.12129>.
- Catchen, J., Hohenlohe, P.A., Bassham, S., Amores, A., Cresko, W.A., 2013. Stacks: An analysis tool set for population genomics. *Mol. Ecol.* 22 (11), 3124–3140. <https://doi.org/10.1111/mec.12354>.
- Che, J., Zhou, W.W., Hu, J.S., Yan, F., Papenfuss, T.J., Wake, D.B., Zhang, Y.P., 2010. Spiny frogs (Paini) illuminate the history of the Himalayan region and Southeast Asia. *Proc. Natl. Acad. Sci.* 107 (31), 13765–13770. <https://doi.org/10.1073/pnas.1008415107>.
- Crayn, D.M., Costion, C., Harrington, M.G., 2015. The Sahul-Sunda floristic exchange: dated molecular phylogenies document Cenozoic intercontinental dispersal dynamics. *J. Biogeogr.* 42 (1), 11–24. <https://doi.org/10.1111/jbi.12405>.
- Dixit, N.M., Zirpel, M., Slik, J.W.F., Jamsari, J., Weising, K., Guicking, D., 2023. Biogeography of the Sunda Shelf revisited: Insights from section *Pruinosae* (Euphorbiaceae). *Front. Ecol. Evol.* 10. <https://doi.org/10.3389/fevo.2022.1049243>.
- Dray, S., Dufour, A.B., Chessel, D., 2007. The ade4 package-II: two-table and K-table methods. *R News* 7 (2), 47–52.
- Elith, J., Phillips, S.J., Hastie, T., Dudík, M., Chee, Y.E., Yates, C.J., 2011. A statistical explanation of MaxEnt for ecologists. *Divers. Distrib.* 17 (1), 43–57. <https://doi.org/10.1111/j.1472-4642.2010.00725.x>.
- Excoffier, L., Lischer, H.E.L., 2010. Arlequin suite ver 3.5: a new series of programs to perform population genetics analyses under Linux and Windows. *Mol. Ecol. Resour.* 10 (3), 564–567. <https://doi.org/10.1111/j.1755-0998.2010.02847.x>.
- Fitak, R.R., 2021. OptM: estimating the optimal number of migration edges on population trees using Treemix. *Biol. Methods Protoc.* 6 (1), bpab017. <https://doi.org/10.1093/biomet/bpab017>.
- Gao, J., Tomlinson, K.W., Zhao, W., Wang, B.S., Lapuz, R.S., Liu, J.X., Pasión, B.O., Hai, B.T., Chanthayod, S., Chen, J., Wang, X.R., 2023. Phylogeography and introgression between *Pinus kesiya* and *Pinus yunnanensis* in Southeast Asia. *J. Syst. Evol.* 62, 120–134. <https://doi.org/10.1111/jse.12949>.
- Gao, Y., Wang, Y., Morley, C.K., Wang, Y., Qian, X., Wang, Y., 2024. Cenozoic thermal-tectonic evolution of Sundaland: constraints from low-temperature thermochronology. *Earth Sci. Rev.* 254, 104812. <https://doi.org/10.1016/j.earscirev.2024.104812>.
- Grimsson, F., Grimm, G.W., Zetter, R., Denk, T., 2016. Cretaceous and Paleogene Fagaceae from North America and Greenland: evidence for a late cretaceous split between *Fagus* and the remaining Fagaceae. *Acta Palaeobot.* 56 (2), 247–305. <https://doi.org/10.1515/acpa-2016-0016>.
- Hall, R., 2009. Southeast Asia's changing palaeogeography. *Blumea* 54 (1–3), 148–161. <https://doi.org/10.3767/000651909x475941>.
- Hall, R., 2012. Late Jurassic-Cenozoic reconstructions of the Indonesian region and the Indian Ocean. *Tectonophysics* 570, 1–41. <https://doi.org/10.1016/j.tecto.2012.04.021>.
- Hall, R., 2013. The palaeogeography of Sundaland and Wallacea since the late Jurassic. *J. Limnol.* 72 (s2), 1–17. <https://doi.org/10.4081/jlimnol.2013.s2.e1>.
- Hijmans, R.J., 2024. Introduction to the “Geosphere” Package (Version 1.5–20). <https://cloud.r-project.org/web/packages/geosphere/vignettes/geosphere.pdf>.
- Hu, L., Le, X.G., Zhou, S.S., Zhang, C.Y., Tan, Y.H., Ren, Q., Meng, H.H., Cun, Y., Li, J., 2022. Conservation significance of the rare and endangered tree species, *Trigonobalanus doichangensis* (Fagaceae). *Diversity* 14 (8), 666. <https://doi.org/10.3390/d14080666>.
- Hu, L., Zhang, X.Y., Song, Y.G., Low, S.L., Xiao, S.M., Zhou, S.S., Li, L., Tan, Y.H., Meng, H.H., Li, J., 2025. Different responses of two endangered sister tree species to climate change: a comparison between island and continental populations in tropical Asia. *Integr. Conserv.* 4 (1), 95–106. <https://doi.org/10.1002/inc3.70005>.
- Huang, P.H., Song, Y.G., Li, J., Meng, H.H., 2025. Did Hainan Island (Southern China) undergo significant cenozoic tectonic displacement, and impact its biota's sourcing and evolution? *J. Biogeogr.* 52 (8), e15168. <https://doi.org/10.1111/jbi.15168>.
- Huang, P.H., Wang, T.R., Li, M., Lu, Z.J., Su, R.P., Fang, O.Y., Li, L., Zhou, S.S., Tan, Y.H., Meng, H.H., Song, Y.G., Li, J., 2024. RAD-seq data for *Engelhardia roxburghiana* provides insights into the palaeobiogeography of Hainan Island and its relationship to mainland China since the late Eocene. *Palaeogeogr. Palaeoclimatol. Palaeoecol.* 651, 112392. <https://doi.org/10.1016/j.palaeo.2024.112392>.
- Hughes, A.C., 2017. Understanding the drivers of Southeast Asian biodiversity loss. *Ecosphere* 8 (1), e01624. <https://doi.org/10.1002/ecs2.1624>.
- Huo, H., Sun, C., 2024. Potential distribution of *Pinus yunnanensis* in Southwest China under climate Change. *J. Sichuan Agric. Univ.* 42 (2), 371–377. <https://doi.org/10.16036/j.issn.1000-2650.202304320>.
- Husson, L., Boucher, F.C., Sarr, A.C., Sepulchre, P., Cahyarini, S.Y., 2020. Evidence of Sundaland's subsidence requires revisiting its biogeography. *J. Biogeogr.* 47 (4), 843–853. <https://doi.org/10.1111/jbi.13762>.
- Husson, L., Salles, T., Lebatard, A.E., Zerathe, S., Braucher, R., Noerwidi, S., Aribowo, S., Mallard, C., Carcaillet, J., Natawidjaja, D.H., Bourles, D., Team, A., 2022. Javanese *Homo erectus* on the move in SE Asia circa 1.8 Ma. *Sci. Rep.* 12, 19012. <https://doi.org/10.1038/s41598-022-23206-9>.
- Jiang, C., Tan, K., Ren, M.X., 2017. Effects of monsoon on distribution patterns of tropical plants in Asia. *Chin. J. Plant Ecol.* 41 (10), 1103–1112. <https://doi.org/10.17521/cjpe.2017.0070>.
- Kellee, K., 2016. Biodiversity Hotspots Map (English labels) (2016.1). Zenodo. <https://doi.org/10.5281/zenodo.4311850>.
- Kopelman, N.M., Mayzel, J., Jakobsson, M., Rosenberg, N.A., Mayrose, I., 2015. Clumpak: a program for identifying clustering modes and packaging population structure inferences across *K*. *Mol. Ecol. Resour.* 15 (5), 1179–1191. <https://doi.org/10.1111/1755-0998.12387>.
- Korneliussen, T.S., Albrechtsen, A., Nielsen, R., 2014. ANGSD: analysis of next generation sequencing data. *BMC Bioinform.* 15 (1). <https://doi.org/10.1186/s12859-014-0356-4>.
- Kuhnhäuser, B.G., Bates, C.D., Dransfield, J., Geri, C., Henderson, A., Julia, S., Lim, J.Y., Morley, R.J., Rustamli, H., Schley, R.J., Bellot, S., Chomicki, G., Eiserhardt, W.L., Hiscock, S.J., Baker, W.J., 2025. Island geography drives evolution of rattan palms in tropical Asian rainforests. *Science* 387 (6739), 1204–1209. <https://doi.org/10.1126/science.adp3437>.
- Li, H., 2013. Aligning sequence reads, clone sequences and assembly contigs with BWA-MEM. *Genomics* 103, 3997. <https://doi.org/10.48550/arXiv.1303.3997>.
- Li, F.Y., Li, S.Q., 2018. Paleocene-Eocene and Plio-Pleistocene Sea-level changes as “species pumps” in Southeast Asia: evidence from spiders. *Mol. Phylogenet. Evol.* 127, 545–555. <https://doi.org/10.1016/j.ympev.2018.05.014>.
- Li, Y.L., Liu, J.X., 2018. StructureSelector: a web-based software to select and visualize the optimal number of clusters using multiple methods. *Mol. Ecol. Resour.* 18 (1), 176–177. <https://doi.org/10.1111/1755-0998.12719>.
- Li, H., Handsaker, B., Wysoker, A., Fennell, T., Ruan, J., Homer, N., Marth, G., Abecasis, G., Durbin, R., Subgroup, G.P.D.P., 2009. The sequence alignment/map format and SAMtools. *Bioinformatics* 25 (16), 2078–2079. <https://doi.org/10.1093/bioinformatics/btp352>.
- Li, X.J., Wang, Z., Yao, Y.J., Gao, H.F., Zhu, S., Xu, Z.Y., 2020. The formation and evolution of the South China Sea. *China Geol.* 47, 1310–1322. <https://doi.org/10.12029/gc20200502>.
- Li, X.J., Wang, Z., Yao, Y.J., Gao, H.F., Zhu, S., Xu, Z.Y., 2023. Formation and evolution of the South China Sea since the late Mesozoic: a review. *China Geol.* 6, 154–167. <https://doi.org/10.31035/cg2022021>.
- Li, M., Wu, J.J., Su, R.P., Fang, O.Y., Cai, X., Huang, P.H., Gao, X.Y., Fu, X.X., Ma, X.H., He, L.Y., Song, Y.G., Hu, G.X., Zhou, S.S., Tan, Y.H., Van der Peer, Y., Li, J., Wu, S.D., Meng, H.H., 2025. Genome analyses provide insights into *Engelhardia*'s adaptation to East Asia Summer Monsoon. *Plant Divers.* 47 (5), 718–732.
- Lim, H.C., Shakya, S.B., Harvey, M.G., Moyle, R.G., Fleischer, R.C., Braun, M.J., Sheldon, F.H., 2020. Opening the door to greater phylogeographic inference in Southeast Asia: Comparative genomic study of five codistributed rainforest bird species using target capture and historical DNA. *Ecol. Evol.* 10 (7), 3222–3247. <https://doi.org/10.1002/ece3.5964>.
- Lin, J.Y., Ng, C.C., Zhuang, X.Y., Mo, L.J., Wang, C.D., Su, W.B., Chen, Q., Chen, W., 2007. Community characteristics and conservation of *Trigonobalanus verticillata* (Fagaceae) on Yinggeling, Hainan Island. *Acta Ecol.* Sin. 27 (6), 2230–2238.
- Lischer, H.E., Excoffier, L., 2012. PGDSpider: an automated data conversion tool for connecting population genetics and genomics programs. *Bioinformatics* 28 (2), 298–299. <https://doi.org/10.1093/bioinformatics/btr642>.
- Liu, X.M., Fu, Y.X., 2020. Stairway Plot 2: demographic history inference with folded SNP frequency spectra. *Genome Biol.* 21, 280. <https://doi.org/10.1186/s13059-020-02196-9>.
- Lohman, D.J., de Bruyn, M., Page, T., von Rintelen, K., Hal, R., Ng, P.K.L., Shih, H.T., Carvalho, G.R., von Rintelen, T., 2011. Biogeography of the Indo-Australian Archipelago. *Annu. Rev. Ecol. Evol. Syst.* 42, 205–226. <https://doi.org/10.1146/annurev-ecolsys-102710-145001>.
- Loria, S.F., Ehrenthal, V.L., Nguyen, A.D., Prendini, L., 2022. Climate relicts: Asian Scorpion family pseudochactidae survived miocene aridification in caves of the annamite mountains. *Insect Syst. Divers.* 6 (6). <https://doi.org/10.1093/isd/ixac028>.
- Luo, Y., Li, S., 2018. Cave Stedocys spitting spiders illuminate the history of the Himalayas and Southeast Asia. *Ecography* 41 (2), 414–423. <https://doi.org/10.1111/ecog.02908>.
- Luo, Y., Li, S., 2022. The stepwise Indian-Eurasian collision and uplift of the Himalayan-Tibetan plateau drove the diversification of high-elevation *Scytodes* spiders. *Cladistics* 38 (5), 582–594. <https://doi.org/10.1111/cla.12512>.
- Luo, T., Zhao, X.R., Lan, C.T., Li, W., Deng, H.Q., Xiao, N., Zhou, J., 2023. Integrated phylogenetic analyses reveal the evolutionary, biogeographic, and diversification history of Asian warty treefrog genus *Theloderma* (Anura, Rhacophoridae). *Ecol. Evol.* 13 (12), e10829. <https://doi.org/10.1002/ee3.10829>.
- Mays, H.L., Hung, C.M., Shaner, P.J., Denvir, J., Justice, M., Yang, S.F., Roth, T.L., Oehler, D.A., Fan, J., Rekulapally, S., Primerano, D.A., 2018. Genomic analysis of demographic history and ecological niche modeling in the endangered Sumatran

- rhinoceros *Dicerorhinus sumatrensis*. Curr. Biol. 28 (1), 70–76. <https://doi.org/10.1016/j.cub.2017.11.021>.
- Meng, H.H., Song, Y.G., 2023. Biogeographic patterns in Southeast Asia: retrospectives and perspectives. Biodivers. Sic. 31 (12), 23261. <https://doi.org/10.17520/biods.2023261>.
- Meng, H.H., Zhou, S.S., Li, L., Tan, Y.H., Li, J.W., Li, J., 2019. Conflict between biodiversity conservation and economic growth: insight into rare plants in tropical China. Biodivers. Conserv. 28 (2), 523–537. <https://doi.org/10.1007/s10531-018-1661-4>.
- Meng, H.H., Gao, X.Y., Song, Y.G., Cao, G.L., Li, J., 2021. Biodiversity arks in the Anthropocene. Reg. Sustain. 2, 109–115. <https://doi.org/10.1016/j.regsus.2021.03.001>.
- Meng, H.H., Song, Y.G., Hu, G.X., Huang, P.H., Li, M., Fang, O.Y., Su, R.P., Cao, G.L., Cai, X., Zhou, S.S., Tan, Y.H., Xiang, X.G., Wang, W., Zhou, Z.K., Li, J., 2025. Evolution of East Asian subtropical evergreen broad-leaved forests: when and how. J. Syst. Evol. 63 (5), 1045–1060. <https://doi.org/10.1111/jse.70001>.
- Meng, H.H., Zhang, C.Y., Song, Y.G., Yu, X.Q., Cao, G.L., Li, L., Cai, C.N., Xiao, J.H., Zhou, S.S., Tan, Y.H., Li, J., 2022. Opening a door to the spatiotemporal history of plants from the tropical Indochina Peninsula to subtropical China. Mol. Phylogenet. Evol. 171, 107458. <https://doi.org/10.1016/j.ympev.2022.107458>.
- Metcalfe, I., 2013. Tectonic evolution of the Malay Peninsula. J. Asian Earth Sci. 76, 195–213. <https://doi.org/10.1016/j.jseas.2012.12.011>.
- Morley, R.J., 1998. Palynological evidence for Tertiary plant dispersals in the SE Asian region in relation to plate tectonics and climate. In: Hall, R., Holloway, J.D. (Eds.), *Biogeography and Geological Evolution of SE Asia*, pp. 211–234.
- Morley, R.J., 2018. Assembly and division of the South and South-East Asian flora in relation to tectonics and climate change. J. Trop. Ecol. 34, 209–234. <https://doi.org/10.1017/S0266467418000202>.
- Nie, X.H., Yan, B.Q., Liu, S., Chu, S.H., Fang, K.F., Liu, Y., Qin, L., Xing, Y., 2024. Molecular genetic analysis of natural introgression to enhance chestnut blight resistance of *Castanea henryi* var. *omeiensis*. Ind. Crop. Prod. 215, 118660. <https://doi.org/10.1016/j.indcrop.2024.118660>.
- Ortego, J., Gugger, P.F., Sork, V.L., 2015. Climatically stable landscapes predict patterns of genetic structure and admixture in the Californian canyon live oak. J. Biogeogr. 42 (2), 328–338. <https://doi.org/10.1111/jbi.12419>.
- Pickrell, J.K., Pritchard, J.K., 2012. Inference of population splits and mixtures from genome-wide allele frequency data. PLoS Genet. 8 (11), e1002967. <https://doi.org/10.1371/journal.pgen.1002967>.
- Purcell, S., Neale, B., Todd-Brown, K., Thomas, L., Ferreira, M.A., Bender, D., Maller, J., Sklar, P., De Bakker, P.I., Daly, M.J., Sham, P.C., 2007. PLINK: a tool set for whole-genome association and population-based linkage analyses. Am. J. Hum. Genet. 81 (3), 559–575. <https://doi.org/10.1086/519795>.
- Quek, S.P., Davies, S.J., Ashton, P.S., Itino, T., Pierce, N.E., 2007. The geography of diversification in mutualistic ants: a gene's-eye view into the Neogene history of Sundaland rain forests. Mol. Ecol. 16 (10), 2045–2062. <https://doi.org/10.1111/j.1365-294X.2007.03294.x>.
- Rambaut, A., Drummond, A.J., Xie, D., Baele, G., Suchard, M.A., 2018. Posterior summarization in bayesian phylogenetics using Tracer 1.7. Syst. Biol. 67 (5), 901–904. <https://doi.org/10.1093/sysbio/syy032>.
- Sadowski, E.M., Schmidt, A.R., Denk, T., 2020. Staminate inflorescences with pollen from Eocene Baltic amber reveal high diversity in (oak family). Willdenowia 50 (3), 405–517. <https://doi.org/10.3372/wi.50.50303>.
- Salgotra, R.K., Chauhan, B.S., 2023. Genetic diversity, conservation, and utilization of plant genetic resources. Genes 14 (1), 174. <https://doi.org/10.3390/genes14010174>.
- Salles, T., Mallard, C., Husson, L., Zahirovic, S., Sarr, A.C., Sepulchre, P., 2021. Quaternary landscape dynamics boosted species dispersal across Southeast Asia. Commun. Earth Environ. 2, 240. <https://doi.org/10.1038/s43247-021-00311-7>.
- Segelbacher, G., Strand, T.M., Quintela, M., Axelsson, T., Jansman, H.A.H., Koelewijn, H.P., Höglund, J., 2014. Analyses of historical and current populations of black grouse in Central Europe reveal strong effects of genetic drift and loss of genetic diversity. Conserv. Genet. 15 (5), 1183–1195. <https://doi.org/10.1007/s10592-014-0610-3>.
- Shaney, K.J., Maldonado, J., Smart, U., Thammachoti, P., Fujita, M., Hamidy, A., Kurniawan, N., Harvey, M.B., Smith, E.N., 2020. Phylogeography of montane dragons could shed light on the history of forests and diversification processes on Sumatra. Mol. Phylogenet. Evol. 149, 106840. <https://doi.org/10.1016/j.ympev.2020.106840>.
- Stamatakis, A., 2014. RAxML version 8: a tool for phylogenetic analysis and post-analysis of large phylogenomes. Bioinformatics 30 (9), 1312–1313. <https://doi.org/10.1093/bioinformatics/btu033>.
- Su, N., Hodel, R.G.J., Wang, X., Wang, J.R., Xie, S.Y., Gui, C.X., Zhang, L., Chang, Z.Y., Zhao, L., Potter, D., Wen, J., 2023. Molecular phylogeny and inflorescence evolution of *Prunus* (Rosaceae) based on RAD-seq and genome skimming analyses. Plant Divers. 45, 397–408. <https://doi.org/10.1016/j.pld.2023.03.013>.
- Suchard, M.A., Lemey, P., Baele, G., Ayres, D.L., Drummond, A.J., Rambaut, A., 2018. Bayesian phylogenetic and phylodynamic data integration using BEAST 1.10. Virus Evol. 4 (1). <https://doi.org/10.1093/ve/vey016>.
- Tan, K., Pastor, L.M., Ren, M., 2020. Origin and evolution of biodiversity hotspots in Southeast Asia. Acta Ecol. Sin. 40 (11), 3866–3877. <https://doi.org/10.5846/stxb201904160762>.
- Tang, W., Xie, X.J., Wang, Y.B., Xiong, L.Q., Guo, J., Li, X., 2024. Evolution of Cenozoic sedimentary architecture in Central and Southern South China Sea basins. J. Palaeogeogr. 13, 35–53. <https://doi.org/10.1016/j.jop.2023.11.001>.
- Voris, H.K., 2000. Maps of Pleistocene Sea levels in Southeast Asia: shorelines, river systems and time durations. J. Biogeogr. 27 (5), 1153–1167. <https://doi.org/10.1046/j.1365-2699.2000.00489.x>.
- Wang, E., Van Wijk, R.E., Braun, M.S., Wink, M., 2017. Gene flow and genetic drift contribute to high genetic diversity with low phylogeographical structure in European hoopoes (*Upupa epops*). Mol. Phylogenet. Evol. 113, 113–125. <https://doi.org/10.1016/j.ympev.2017.05.018>.
- Wang, J., Tian, S., Sun, X., Cheng, X., Duan, N., Tao, J., Shen, G., 2020. Construction of Pseudomolecules for the Chinese Chestnut (*Castanea mollissima*). Genome. G3 (Bethesda) 10 (10), 3565–3574. <https://doi.org/10.1534/g3.120.401532>.
- Whitlock, M.C., McCauley, D.E., 1999. Indirect measures of gene flow and migration:  $FST/(4Nm+1)$ . Natur. 82, 117–123. <https://doi.org/10.1038/sj.nature.6884960>.
- Whittaker, R.J., Fernández-Palacios, J.M., Matthews, T.J., Borregaard, M.K., Triantis, K.A., 2017. Island biogeography: taking the long view of nature's laboratories. Science 357 (6354), eaam8326. <https://doi.org/10.1126/science.aam8326>.
- Wickham, H., 2016. *ggplot2: Elegant Graphics for Data Analysis*. Springer, New York.
- Wielstra, B., Salvi, D., Canestrelli, D., 2021. Genetic divergence across Glacial Refugia despite interglacial gene flow in a Crested Newt. Evol. Biol. 48, 17–26. <https://doi.org/10.1007/s11692-020-09519-5>.
- Wurster, C.M., Bird, M.I., Bull, I.D., Creed, F., Bryant, C., Dungait, J.A.J., Paz, V., 2010. Forest contraction in north equatorial Southeast Asia during the last Glacial Period. Proc. Natl. Acad. Sci. USA 107 (35), 15508–15511. <https://doi.org/10.1073/pnas.1005507107>.
- Xia, X.H., 2019. PGT: visualizing temporal and spatial biogeographic patterns. Glob. Ecol. Biogeogr. 28 (8), 1195–1199. <https://doi.org/10.1111/geb.12914>.
- Yi, X., Latch, E.K., 2022. Nuclear phylogeography reveals strong impacts of gene flow in big brown bats. J. Biogeogr. 49, 1061–1074. <https://doi.org/10.1111/jbi.14362>.
- Yu, Y., Blair, C., He, X., 2019. RASP 4: ancestral state reconstruction tool for multiple genes and characters. Mol. Biol. Evol. 37 (2), 604–606. <https://doi.org/10.1093/molbev/msz257>.
- Yu, Y.L., Wang, H.C., Yu, Z.X., Schinnerl, J., Tang, R., Geng, Y.P., Chen, G., 2021. Genetic diversity and structure of the endemic and endangered species *Aristolochia delavayi* growing along the Jinsha River. Plant Divers. 43 (3), 225–233. <https://doi.org/10.1016/j.jpld.2020.12.007>.
- Zhang, Y., Wang, G., Zhuang, H., Wang, L., Innes, J.L., Ma, K., 2021. Integrating hotspots for endemic, threatened and rare species supports the identification of priority areas for vascular plants in SW China. For. Ecol. Manag. 484, 118952. <https://doi.org/10.1016/j.foreco.2021.118952>.
- Zhang, L.G., Li, X.Q., Jin, W.T., Liu, Y.J., Yao Zhao, Y., Rong, J., Xiang, X.G., 2023. Asymmetric migration dynamics of the tropical Asian and Australasian floras. Plant Divers. 2023 (45), 20–26. <https://doi.org/10.1016/j.jpld.2022.05.006>.
- Zhang, L., Liang, Z.L., Fan, X.P., Lu, N.T., Zhou, X.M., Wei, H.J., Zhang, L.B., 2024. The Indo-Burma biodiversity hotspot for ferns: Updated phylogeny, hidden diversity, and biogeography of the java fern genus *Leptochilus* (Polypodiaceae). Plant Divers. 2024 (46), 698–712. <https://doi.org/10.1016/j.jpld.2024.08.005>.
- Zhang, C.Y., Cao, G.L., Hu, J.L., Huang, P.H., Li, M., Su, R.P., Fang, O.Y., Cai, X., Song, Y.G., Hu, G.X., Xie, K.Q., Li, L., Zhou, S.S., Tan, Y.H., Meng, H.H., Li, J., 2025. The reconstructed evolutionary history of the *Engelhardia spicata* complex highlights the impact of a three-tiered landform in the Indo-Burma ecoregion. Am. J. Bot. 112, e70077. <https://doi.org/10.1002/ajb2.70077>.
- Zhao, Y.J., Shen Yin, G.S., Gong, X., 2023. RAD-sequencing improves the genetic characterization of a threatened tree peony (*Paeonia ludlowii*) endemic to China: implications for conservation. Plant Divers. 45, 513–522. <https://doi.org/10.1016/j.jpld.2022.07.002>.
- Zhou, B.F., Yuan, S., Crowl, A.A., Liang, Y.Y., Shi, Y., Chen, X.Y., An, Q.Q., Kang, M., Manos, P.S., Wang, B., 2022. Phylogenomic analyses highlight innovation and introgression in the continental radiations of Fagaceae across the Northern Hemisphere. Nat. Commun. 13 (1), 1320. <https://doi.org/10.1038/s41467-022-28917-1>.
- Ziegler, T., Luu, V.Q., Nguyen, T.T., Ha, N.V., Ngo, H.T., Le, M.D., Nguyen, T.Q., 2019. Rediscovery of Andreae's keelback, (Ziegler & Le, 2006): first country record for Laos and phylogenetic placement. Rev. Suisse Zool. 126 (1), 61–71. <https://doi.org/10.5281/zenodo.2619520>.